Author(s): Hinkkanen, Marko & Tuovinen, Toni & Harnefors, Lennart & Luomi, Jorma

Title: A reduced-order position observer with stator-resistance adaptation for PMSM drives

Year: 2010

Version: Post print

**Please cite the original version:**

Hinkkanen, Marko & Tuovinen, Toni & Harnefors, Lennart & Luomi, Jorma. 2010. A reduced-order position observer with stator-resistance adaptation for PMSM drives. 2010 IEEE International Symposium on Industrial Electronics (ISIE). 6. ISBN 978-1-4244-6390-9 (printed). DOI: 10.1109/isie.2010.5637851.

# A Reduced-Order Position Observer with Stator-Resistance Adaptation for PMSM Drives

Marko Hinkkanen*, Toni Tuovinen*, Lennart Harnefors†, and Jorma Luomi*
*Aalto University School of Science and Technology
Department of Electrical Engineering, P.O. Box 13000, FI-00076 Aalto, Finland
†ABB Power Systems, PSDC/DCTU, SE-77180 Ludvika, Sweden

***Abstract*—A reduced-order position observer with stator-resistance adaptation is proposed for motion-sensorless permanent-magnet synchronous motor drives. A general analytical solution for the stabilizing observer gain and stability conditions for the stator-resistance adaptation are derived. Under these conditions, the local stability of the position and stator-resistance estimation is guaranteed at every operating point except the zero frequency, if other motor parameters are known. The proposed observer design is experimentally tested using a 2.2-kW motor drive; stable operation at very low speeds under different loading conditions is demonstrated.**

***Index Terms*—Observer, stability conditions, speed sensorless, stator resistance estimation.**

## I. Introduction

Permanent-magnet synchronous motor (PMSM) drives are becoming more and more popular in a wide area of applications due to their dynamic performance, efficiency, and high torque density. In low-cost applications, motion-sensorless operation of the drive is preferred, and signal-injection methods are avoided in order to minimize hardware costs. Hence, a robust and easy-to-tune rotor-position observer, based only on the fundamental excitation, is needed [1]–[6].

Even if the drive is equipped with a motion sensor, a sensorless-control mode can be beneficial, for example, as a fallback strategy in the case of sensor failure. In some applications, a position observer can be augmented with a signal-injection method for low-speed operation [7], [8], [9]; it is important that the underlying fundamental-excitation-based observer is stable and well-damped in the whole speed and load range.

Motion-sensorless PMSM drives may have unstable operating regions at low speeds, especially if the saliency ratio of the machine is high. Since the back electromotive force (EMF) is proportional to the rotational speed of the motor, parameter errors have a relatively high effect on the accuracy of the estimated back EMF at low speeds [4]. Improper observer gain selections may cause unstable operation of the drive even if the parameters are accurately known [3], [5].

In practice, the stator resistance varies with the winding temperature during the operation of the motor. The stator resistance can be estimated by injecting a test signal into the stator winding, or by using the fundamental excitation in combination with a machine model. For PMSMs, a dc-current signal has been used for identifying the stator resistance in [10]. A combination of steady-state equations and the response to an alternating-current signal has been used in [11]. In [12], [13], a model-reference adaptive system (MRAS) is applied for on-line stator resistance estimation in order to improve the sensorless control. Usually, an in-depth stability analysis of these methods is omitted since the resulting closed-loop systems become very complicated.

The main contributions of this paper are:

1) A reduced-order observer is proposed for PMSM drives.
2) Analytical stability conditions are derived and formulated as a general stabilizing gain, which simplifies the tuning procedure.
3) The proposed observer is augmented with the stator-resistance adaptation, and the analytical stability conditions are derived for the augmented observer.
4) An easy-to-tune observer design is proposed.

The proposed design is comparatively simple, and it results in a robust and well-damped closed-loop system. If desired, the observer could be augmented with a signal-injection method, for example in a fashion similar to [7]. The performance of the proposed observer design is evaluated using laboratory experiments with a 2.2-kW PMSM drive.

## II. PMSM Model

Real space vectors will be used throughout the paper. For example, the stator-current vector is $\boldsymbol{i}_\mathrm{s} = [i_\mathrm{d}, i_\mathrm{q}]^\mathrm{T}$, where $i_\mathrm{d}$ and $i_\mathrm{q}$ are the components of the vector and the matrix transpose is marked with the superscript T. The identity matrix and the orthogonal rotation matrix are defined as

$$\mathbf{I} = \begin{bmatrix} 1 & 0 \\ 0 & 1 \end{bmatrix}, \quad \mathbf{J} = \begin{bmatrix} 0 & -1 \\ 1 & 0 \end{bmatrix}$$

respectively.

The electrical position of the permanent-magnet flux is denoted by $\vartheta_\mathrm{m}$. The position depends on the electrical angular rotor speed $\omega_\mathrm{m}$ according to

$$\frac{\mathrm{d}\vartheta_\mathrm{m}}{\mathrm{d}t} = \omega_\mathrm{m} \tag{1a}$$

To simplify the analysis in the following sections, the machine model will be expressed in the *estimated* rotor reference frame, whose d axis is aligned at $\hat{\vartheta}_\mathrm{m}$ with respect to the stator reference frame. The stator inductance and the permanent-magnet-flux vector are

$$\boldsymbol{L} = \mathrm{e}^{-\tilde{\vartheta}_\mathrm{m}\mathbf{J}} \begin{bmatrix} L_\mathrm{d} & 0 \\ 0 & L_\mathrm{q} \end{bmatrix} \mathrm{e}^{\tilde{\vartheta}_\mathrm{m}\mathbf{J}}, \quad \boldsymbol{\psi}_\mathrm{pm} = \mathrm{e}^{-\tilde{\vartheta}_\mathrm{m}\mathbf{J}} \begin{bmatrix} \psi_\mathrm{pm} \\ 0 \end{bmatrix} \tag{1b}$$

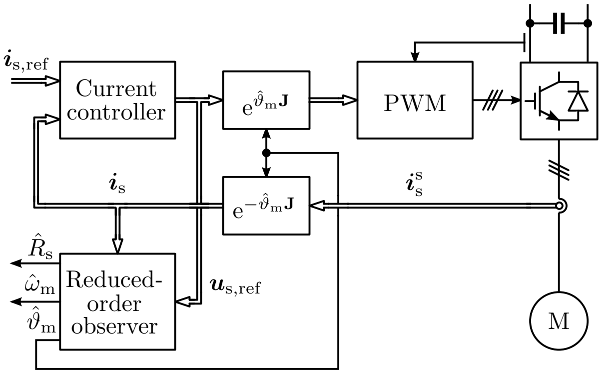


Fig. 1. Speed-sensorless rotor-oriented controller. The observer is implemented in the estimated rotor coordinates.

respectively, where $\tilde{\vartheta}_{\mathrm{m}} = \hat{\vartheta}_{\mathrm{m}} - \vartheta_{\mathrm{m}}$ is the estimation error in the rotor position, $L_{\mathrm{d}}$ the direct-axis inductance, $L_{\mathrm{q}}$ the quadrature-axis inductance, and $\psi_{\mathrm{pm}}$ the permanent-magnet flux. The voltage equation is

$$\frac{\mathrm{d}\boldsymbol{\psi}_{\mathrm{s}}}{\mathrm{d}t} = \boldsymbol{u}_{\mathrm{s}} - R_{\mathrm{s}}\boldsymbol{i}_{\mathrm{s}} - \hat{\omega}_{\mathrm{m}}\mathbf{J}\boldsymbol{\psi}_{\mathrm{s}} \tag{1c}$$

where $\boldsymbol{\psi}_{\mathrm{s}}$ is the stator-flux vector, $\boldsymbol{u}_{\mathrm{s}}$ the stator-voltage vector, $R_{\mathrm{s}}$ the stator resistance, and $\hat{\omega}_{\mathrm{m}} = \mathrm{d}\hat{\vartheta}_{\mathrm{m}}/\mathrm{d}t$ is the angular speed of the coordinate system. The stator current is a nonlinear function

$$\boldsymbol{i}_{\mathrm{s}} = \boldsymbol{L}^{-1}(\boldsymbol{\psi}_{\mathrm{s}} - \boldsymbol{\psi}_{\mathrm{pm}}) \tag{1d}$$

of the stator-flux vector and the position error $\tilde{\vartheta}_{\mathrm{m}}$.

## III. Rotor-Position Observer

To avoid forbiddingly complicated equations, which would prevent analytical results from being derived, accurate parameter estimates $L_{\mathrm{d}}$, $L_{\mathrm{q}}$, and $\psi_{\mathrm{pm}}$ are assumed[1], with the exception of the stator-resistance estimate $\hat{R}_{\mathrm{s}}$. Without loss of generality, the observer in estimated rotor coordinates is considered. Since the rotor-position estimation error is unknown, the inductance matrix and permanent-magnet-flux vector estimates are

$$\hat{\boldsymbol{L}} = \begin{bmatrix} L_{\mathrm{d}} & 0 \\ 0 & L_{\mathrm{q}} \end{bmatrix}, \quad \hat{\boldsymbol{\psi}}_{\mathrm{pm}} = \begin{bmatrix} \psi_{\mathrm{pm}} \\ 0 \end{bmatrix} \tag{2}$$

respectively. A typical rotor-oriented control system is depicted in Fig. 1, where the rotor-position estimate $\hat{\vartheta}_{\mathrm{m}}$ is calculated in estimated rotor coordinates.

### A. Adaptive Observer

A conventional method for estimating the rotor position is to apply a speed-adaptive observer [1], [9]

$$\frac{\mathrm{d}\hat{\boldsymbol{\psi}}_{\mathrm{s}}}{\mathrm{d}t} = \boldsymbol{u}_{\mathrm{s}} - \hat{R}_{\mathrm{s}}\boldsymbol{i}_{\mathrm{s}} - \hat{\omega}_{\mathrm{m}}\mathbf{J}\hat{\boldsymbol{\psi}}_{\mathrm{s}} + \boldsymbol{K}(\hat{\boldsymbol{i}}_{\mathrm{s}} - \boldsymbol{i}_{\mathrm{s}}) \tag{3a}$$

$$\frac{\mathrm{d}\hat{\vartheta}_{\mathrm{m}}}{\mathrm{d}t} = \hat{\omega}_{\mathrm{m}} \tag{3b}$$

$$\hat{\boldsymbol{i}}_{\mathrm{s}} = \hat{\boldsymbol{L}}^{-1}(\hat{\boldsymbol{\psi}}_{\mathrm{s}} - \hat{\boldsymbol{\psi}}_{\mathrm{pm}}) \tag{3c}$$

where $\hat{\boldsymbol{\psi}}_{\mathrm{s}} = [\hat{\psi}_{\mathrm{d}}, \hat{\psi}_{\mathrm{q}}]^{\mathrm{T}}$ and the 2×2 matrix $\boldsymbol{K}$ is the observer gain. In order to estimate the rotor speed $\hat{\omega}_{\mathrm{m}}$ and the position $\hat{\vartheta}_{\mathrm{m}}$, the observer (3) has been augmented with a speed-adaptation law. Typically, the estimation error $\hat{i}_{\mathrm{q}} - i_{\mathrm{q}}$ is fed to the PI mechanism whose output is the speed estimate

$$\hat{\omega}_{\mathrm{m}} = k_{\mathrm{p}}(\hat{i}_{\mathrm{q}} - i_{\mathrm{q}}) + k_{\mathrm{i}} \int (\hat{i}_{\mathrm{q}} - i_{\mathrm{q}})\mathrm{d}t \tag{4}$$

The adaptive observer consisting of (3) and (4) is of the fourth order, and there are four parameters to tune (assuming that $\boldsymbol{K}$ is skew-symmetric).

### B. Proposed Reduced-Order Observer

*1) Structure:* The observer order can be reduced by estimating only the d component $\hat{\psi}_{\mathrm{d}}$ while the q component is evaluated based on the measured current. The stator-flux estimate is redefined as

$$\hat{\boldsymbol{\psi}}_{\mathrm{s}} = \begin{bmatrix} \hat{\psi}_{\mathrm{d}} \\ L_{\mathrm{q}} i_{\mathrm{q}} \end{bmatrix} = \begin{bmatrix} L_{\mathrm{d}}\hat{i}_{\mathrm{d}} + \psi_{\mathrm{pm}} \\ L_{\mathrm{q}} i_{\mathrm{q}} \end{bmatrix} \tag{5}$$

Since the q component of the current-estimation error is not available, the observer gain reduces to

$$\boldsymbol{K} = \begin{bmatrix} L_{\mathrm{d}} k_1 & 0 \\ L_{\mathrm{d}} k_2 & 0 \end{bmatrix} \tag{6}$$

where the two gain components $k_1$ and $k_2$ are scaled with $L_{\mathrm{d}}$ for convenience. Using the definitions (5) and (6) in (3), the componentwise presentation of the proposed reduced-order observer becomes

$$\frac{\mathrm{d}\hat{\psi}_{\mathrm{d}}}{\mathrm{d}t} = u_{\mathrm{d}} - \hat{R}_{\mathrm{s}} i_{\mathrm{d}} + \hat{\omega}_{\mathrm{m}} L_{\mathrm{q}} i_{\mathrm{q}} + k_1(\hat{\psi}_{\mathrm{d}} - \psi_{\mathrm{pm}} - L_{\mathrm{d}} i_{\mathrm{d}}) \tag{7a}$$

$$\frac{\mathrm{d}\hat{\vartheta}_{\mathrm{m}}}{\mathrm{d}t} = \frac{u_{\mathrm{q}} - \hat{R}_{\mathrm{s}} i_{\mathrm{q}} - L_{\mathrm{q}}\frac{\mathrm{d}i_{\mathrm{q}}}{\mathrm{d}t} + k_2(\hat{\psi}_{\mathrm{d}} - \psi_{\mathrm{pm}} - L_{\mathrm{d}} i_{\mathrm{d}})}{\hat{\psi}_{\mathrm{d}}} \tag{7b}$$

The rotor speed estimate is obtained directly from (7b) since $\hat{\omega}_{\mathrm{m}} = \mathrm{d}\hat{\vartheta}_{\mathrm{m}}/\mathrm{d}t$. The speed-adaptation law is avoided and the implementation becomes easier. The proposed observer is of the second order and there are only two gains.

*2) Stabilizing Observer Gain:* The gains $k_1$ and $k_2$ determine the stability (and other properties) of the observer. As shown in Appendix A, the closed-loop system consisting of (1) and (7) is locally stable in every operating point if (and only if) the gains are given by[2]

$$k_1 = -\frac{b + \beta(c/\hat{\omega}_{\mathrm{m}} - \hat{\omega}_{\mathrm{m}})}{\beta^2 + 1}, \quad k_2 = \frac{\beta b - c/\hat{\omega}_{\mathrm{m}} + \hat{\omega}_{\mathrm{m}}}{\beta^2 + 1} \tag{8}$$

where the coefficients $b > 0$ and $c > 0$ may depend on the operating point and

$$\beta = \frac{(L_{\mathrm{d}} - L_{\mathrm{q}}) i_{\mathrm{q}}}{\psi_{\mathrm{pm}} + (L_{\mathrm{d}} - L_{\mathrm{q}}) i_{\mathrm{d}}} \tag{9}$$

As a special case, (9) reduces to $\beta = 0$ for non-salient PMSMs.

The observer gain design problem is reduced to the selection of the two positive coefficients $b$ and $c$, which are actually the

[1]In practical implementations, the effect of the magnetic saturation on $L_{\mathrm{d}}$ and $L_{\mathrm{q}}$ can be taken into account using explicit functions or look-up tables.

[2]For $\hat{\omega}_{\mathrm{m}} = 0$, $c = 0$ has to be selected to avoid division by zero, giving only marginal stability for zero speed.

coefficients of the characteristic polynomial of the linearized closed-loop system, cf. Appendix A. Hence, (8) can be used to place the poles of the linearized closed-loop system arbitrarily. An accurate stator-resistance estimate $\hat{R}_\mathrm{s}$ was assumed in the derivation of (8), but this assumption will be lifted, as will be described in Section III-B3.

The stability with accurate parameter estimates is necessary but not a sufficient design goal. In addition, it is typically required that the system should be well damped, robust against parameter errors and noise, and easy to tune. Numerical studies have been carried out to search for the coefficients $b$ and $c$ that would satisfy these criteria. It was found out that the coefficient $b$ can be kept constant while $c = b|\hat{\omega}_\mathrm{m}| + \hat{\omega}_\mathrm{m}^2$ leads to the simple gains

$$k_1 = -b\frac{\beta\,\mathrm{sign}(\hat{\omega}_\mathrm{m}) + 1}{\beta^2+1}, \quad k_2 = b\frac{\beta - \mathrm{sign}(\hat{\omega}_\mathrm{m})}{\beta^2+1} \tag{10}$$

that are independent on the rotor speed estimate (except its sign). This gain selection is an acceptable compromise between design criteria (damping, robustness, and simplicity). If different design criteria are preferred, coeffients $b$ and $c$ could be searched, for example, by means of numerical optimization.

*3) Stator-Resistance Adaptation:* The following stator-resistance adaptation law is proposed:

$$\frac{\mathrm{d}\hat{R}_\mathrm{s}}{\mathrm{d}t} = k_\mathrm{R}(\hat{\psi}_\mathrm{d} - \psi_\mathrm{pm} - L_\mathrm{d} i_\mathrm{d}) \tag{11}$$

where $k_\mathrm{R}$ is the adaptation gain. As shown in Appendix B, the general stability conditions for the observer augmented with (11) are

$$k_\mathrm{R}(i_\mathrm{q} + \beta i_\mathrm{d})\hat{\omega}_\mathrm{m} > 0 \tag{12a}$$

$$k_\mathrm{R}[(i_\mathrm{d} - \beta i_\mathrm{q})b - (i_\mathrm{q} + \beta i_\mathrm{d})\hat{\omega}_\mathrm{m}] + bc > 0 \tag{12b}$$

where $b$ and $c$ are the positive design parameters in (8).

The stability conditions will be applied in the following. Based on the condition (12a), the sign of the gain $k_\mathrm{R}$ has to depend on the operating mode. Furthermore, the magnitude of $k_\mathrm{R}$ has to be limited according to (12b). It can be shown that the conditions in (12) are fulfilled by choosing

$$k_\mathrm{R} = \begin{cases} \min\{k'_\mathrm{R}, L\}, & \text{if } x > 0 \text{ and } L > 0 \\ \max\{-k'_\mathrm{R}, L\}, & \text{if } x < 0 \text{ and } L < 0 \\ k'_\mathrm{R}\,\mathrm{sign}(x), & \text{otherwise} \end{cases} \tag{13}$$

where $k'_\mathrm{R}$ is a positive design parameter. The sign of the gain $k_\mathrm{R}$ is determined by $x = (i_\mathrm{q} + \beta i_\mathrm{d})\hat{\omega}_\mathrm{m}$. The limiting value is

$$L = -r\frac{bc}{(i_\mathrm{d} - \beta i_\mathrm{q})b - (i_\mathrm{q} + \beta i_\mathrm{d})\hat{\omega}_\mathrm{m}} \tag{14}$$

where the parameter $0 < r < 1$ affects the stability margin of the system; choosing $r = 1$ would lead to a marginally stable system (in the operating points where $k_\mathrm{R}$ is determined by $L$).

In practice, the adaptation should be disabled in the vicinity of no-load operation and at higher stator frequencies due to poor signal-to-noise ratio (which is a fundamental property common to all stator-resistance adaptation methods based only on the fundamental-wave excitation). Hence, parameter $k'_\mathrm{R}$ in (13) can be selected as

$$k'_\mathrm{R} = \begin{cases} k''_\mathrm{R}\left(1 - \frac{|\hat{\omega}_\mathrm{m}|}{\omega_\Delta}\right) i_\mathrm{s}, & \text{if } i_\mathrm{s} > i_\Delta \text{ and } |\hat{\omega}_\mathrm{m}| < \omega_\Delta \\ 0, & \text{otherwise} \end{cases} \tag{15}$$

where $k''_\mathrm{R}$, $\omega_\Delta$, and $i_\Delta$ are positive constants, and $i_\mathrm{s}$ is the magnitude of the stator-current vector.

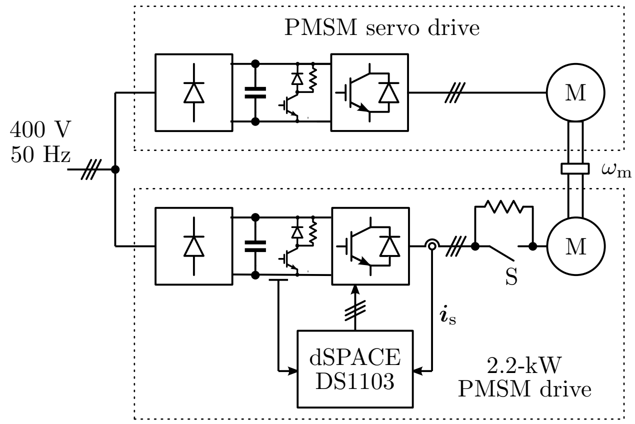


Fig. 2. Experimental setup. The stator currents and the DC-link voltage are used as feedback signals. Mechanical load is provided by a servo drive. The rotor speed $\omega_\mathrm{m}$ is measured for monitoring purposes. Three-phase switch S is in the closed position, except in the experiment shown in Fig. 4.

## IV. Experimental Setup and Parameters

The operation of the proposed observer and stator-resistance adaptation was investigated experimentally using the setup shown in Fig. 2. The motion-sensorless control system was implemented in a dSPACE DS1103 PPC/DSP board. A 2.2-kW six-pole PMSM is fed by a frequency converter that is controlled by the DS1103 board. The rated values of the PMSM are: speed 1500 r/min; frequency 75 Hz; line-to-line rms voltage 370 V; rms current 4.3 A; and torque 14 Nm. The base values for angular speed, voltage, and current are defined as $2\pi \cdot 75$ rad/s, $\sqrt{2/3} \cdot 370$ V, and $\sqrt{2} \cdot 4.3$ A, respectively.

A servo PMSM is used as a loading machine. The rotor speed $\omega_\mathrm{m}$ and position $\vartheta_\mathrm{m}$ are measured using an incremental encoder for monitoring purposes. The total moment of inertia of the experimental setup is 0.015 kgm$^2$ (2.2 times the inertia of the 2.2-kW PMSM rotor).

The stator resistance of the 2.2-kW PMSM is approximately 3.3 Ω at room temperature. Additional 1-Ω resistors were added between the frequency converter and the PMSM. The resistance can be changed stepwise by opening or closing a manually operated three-phase switch (S) connected in parallel with the resistors. Unless otherwise noted, switch S is in the closed position.

The block diagram of the speed-sensorless control system implemented in the DS1103 board is shown in Fig. 1. The stator currents and the DC-link voltage are measured, and the reference voltage obtained from the current controller is used for the observer. The sampling is synchronized to

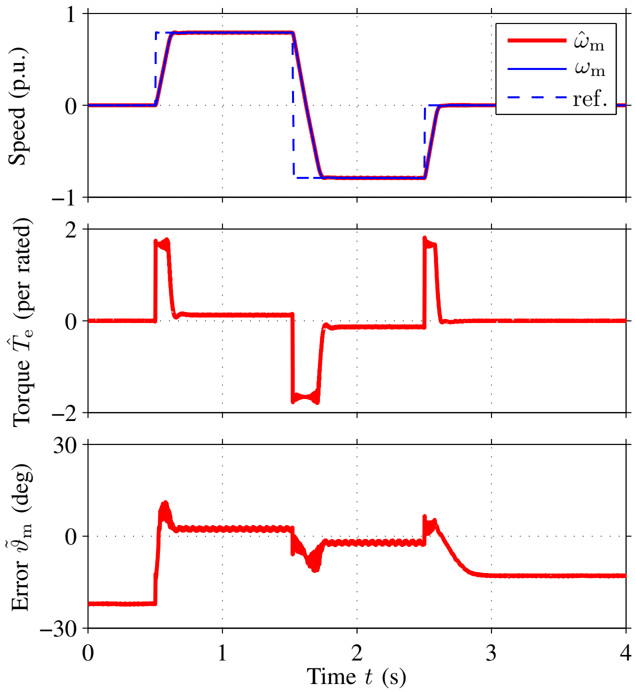


Fig. 3. Experimental results showing speed-reference steps (0 → 1200 rpm → −1200 rpm → 0) at no load.

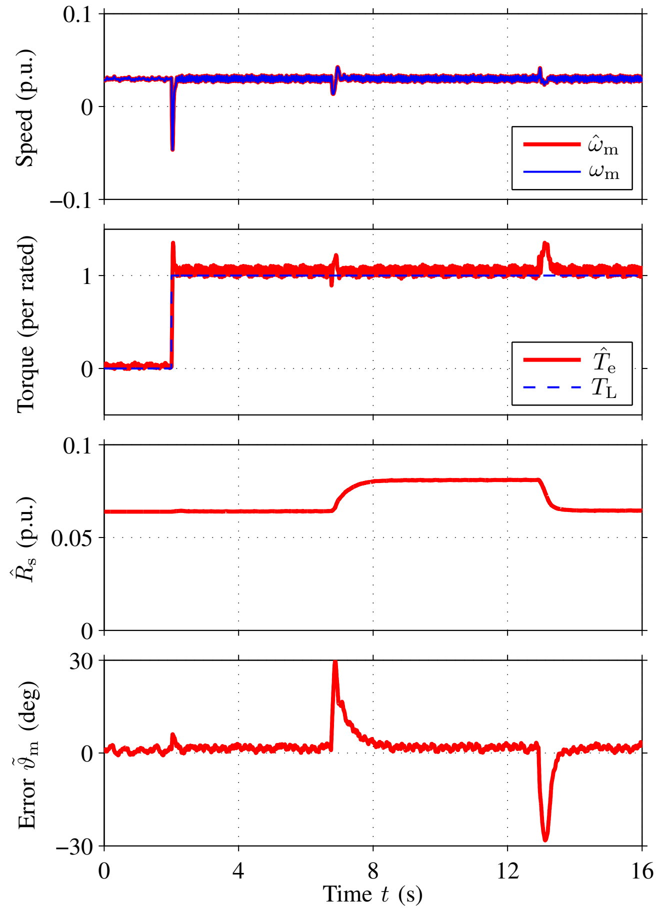


Fig. 4. Experimental results showing the stepwise increase of 1 Ω in the actual stator resistance at $t = 7$ s and the decrease at $t = 13$ s. Speed reference is kept at 45 rpm and a rated load torque is applied at $t = 2$ s. $T_L$ shown in the second subplot is the torque reference of the loading drive.

the modulation, and both the switching frequency and the sampling frequency are 5 kHz. A simple current feedforward compensation for dead times and power device voltage drops is applied. The control system shown in Fig. 1 is augmented with a speed controller, whose feedback signal is the speed estimate $\hat{\omega}_m$ obtained from the proposed observer. The bandwidth of this PI controller, including active damping [14], is 0.08 p.u. The estimate of the per-unit electromagnetic torque is evaluated as $\hat{T}_e = \psi_{pm} i_q + (L_d - L_q) i_d i_q$.

The proposed observer was implemented in the estimated rotor coordinates using (7), (10), (11), (13), and (15). The per-unit parameter estimates used in the experiments are: $L_d = 0.33$ p.u.; $L_q = 0.45$ p.u.; and $\psi_{pm} = 0.895$ p.u. The observer gain (10) is determined by the constant $b = 3$ p.u. The parameters needed for the stator-resistance adaptation are: $r = 0.1$ in (14) and $k''_R = 0.02$ p.u., $\omega_\Delta = 0.25$ p.u., and $i_\Delta = 0.2$ p.u. in (15).

## V. Experimental Results

Fig. 3 shows results of medium-speed no-load operation. The speed reference was stepped from 0 to 1200 rpm, then to −1200 rpm and finally back to 0. According to (15), the stator-resistance adaptation was only active in the beginning of the acceleration and at the end of the deceleration. Even though there is an initial error of approximately 20 electrical degrees in the rotor position estimate, it can be seen that the position estimate quickly converges close to the actual position in the beginning of the acceleration. The position error increases slightly at the end of the deceleration ($t > 2.5$ s) since the stator current, voltage and frequency approach zero and, therefore, there is no information available on the position. However, it is worth noticing that the position estimate remains stable at zero speed and the drive could be accelerated again.

Fig. 4 shows the stepwise change in the stator resistance (as seen by the frequency converter). Initially, three-phase switch S, cf. Fig. 2, was in the closed position. The speed reference was kept at 45 rpm. A rated-load torque step was applied at $t = 2$ s. Switch S was opened at $t = 7$ s, causing a 0.02-p.u. increase (corresponding to 30%) in the actual stator resistance. Switch S was closed at $t = 13$ s. It can be seen that the stator-resistance estimate tracks the change in the actual stator resistance.

Fig. 5 shows load-torque steps when the speed reference was kept at 30 rpm. The load torque was stepped to the rated value at $t = 2.5$ s, reversed at $t = 7.5$ s, and removed at $t = 12.5$ s. It can be seen that the proposed observer behaves well in torque transients.

Results of a slow speed reversals are shown in Fig. 6. A rated-load torque step was applied at $t = 2$ s. The speed reference was slowly ramped from 150 rpm to −150 rpm and back to 150 rpm. During the sequence, the drive operates in

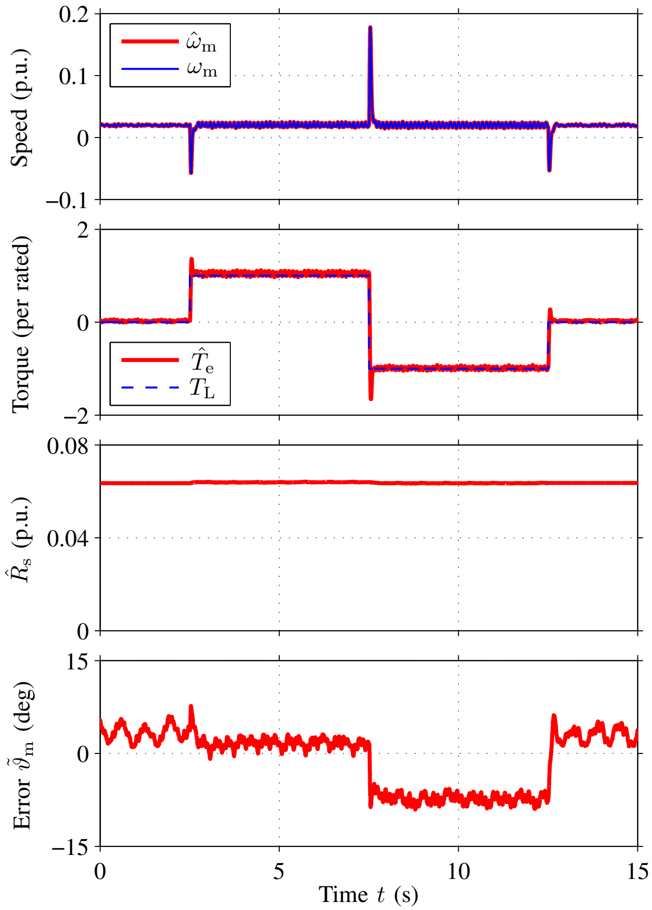


Fig. 5. Experimental results showing load-torque steps (0 → rated → negative rated → 0) when the speed reference is kept at 30 rpm.

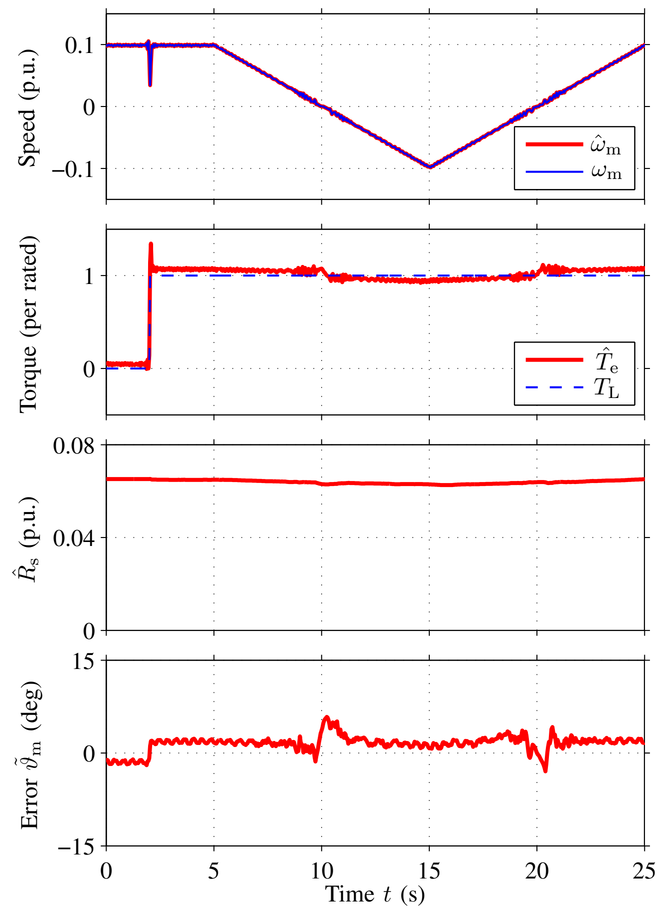


Fig. 6. Experimental results showing slow speed reversals (150 rpm → −150 rpm → 150 rpm) when the rated load torque is applied.

the motoring and regenerating modes. In the vicinity of zero frequency, the rotor-position estimate begins to deviate from the actual position but the system remains stable. Without the stabilizing observer gain, this kind of speed reversals would not be possible. Furthermore, without the stator-resistance adaptation, a very accurate stator-resistance estimate would be needed since the frequency remains in the vicinity of zero for a long time.

## VI. Conclusions

In this paper, a reduced-order position observer with stator-resistance adaptation was proposed for motion-sensorless PMSM drives. A general analytical solution for the stabilizing observer gain and stability conditions for the stator-resistance adaptation were derived. Under these conditions, the local stability of the position and stator-resistance estimation is guaranteed at every operating point except the zero frequency, if other motor parameters are known. The proposed observer design is simple, and it results in a comparatively robust and well-damped closed-loop system. The observer was experimentally tested using a 2.2-kW PMSM drive; stable operation at very low speeds under different loading conditions is demonstrated. Furthermore, it was experimentally verified that the stator-resistance estimate can track stepwise changes in the actual resistance.

## Appendix A
## Derivation of a Stabilizing Observer Gain

From (1) and (3), the nonlinear dynamics of the estimation error are obtained:

$$\frac{\mathrm{d}\tilde{\boldsymbol{\psi}}_\mathrm{s}}{\mathrm{d}t} = \boldsymbol{K}\tilde{\boldsymbol{i}}_\mathrm{s} - \hat{\omega}_\mathrm{m}\mathbf{J}\tilde{\boldsymbol{\psi}}_\mathrm{s} - \tilde{R}_\mathrm{s}\boldsymbol{i}_\mathrm{s} \tag{16a}$$

$$\frac{\mathrm{d}\tilde{\vartheta}_\mathrm{m}}{\mathrm{d}t} = \tilde{\omega}_\mathrm{m} \tag{16b}$$

$$\tilde{\boldsymbol{i}}_\mathrm{s} = \boldsymbol{L}^{-1}\left(\tilde{\boldsymbol{\psi}}_\mathrm{s} - \tilde{\boldsymbol{\psi}}_\mathrm{pm}\right) + \left(\boldsymbol{L}^{-1} - \hat{\boldsymbol{L}}^{-1}\right)\left(\hat{\boldsymbol{\psi}}_\mathrm{s} - \hat{\boldsymbol{\psi}}_\mathrm{pm}\right) \tag{16c}$$

where

$$\tilde{\boldsymbol{\psi}}_\mathrm{pm} = \hat{\boldsymbol{\psi}}_\mathrm{pm} - \boldsymbol{\psi}_\mathrm{pm} = \left(\mathbf{I} - \mathrm{e}^{-\tilde{\vartheta}_\mathrm{m}\mathbf{J}}\right)\begin{bmatrix}\psi_\mathrm{pm} \\ 0\end{bmatrix} \tag{17}$$

and $\tilde{\boldsymbol{\psi}}_\mathrm{s} = \hat{\boldsymbol{\psi}}_\mathrm{s} - \boldsymbol{\psi}_\mathrm{s}$, $\tilde{\vartheta}_\mathrm{m} = \hat{\vartheta}_\mathrm{m} - \vartheta_\mathrm{m}$, and $\tilde{\omega}_\mathrm{m} = \hat{\omega}_\mathrm{m} - \omega_\mathrm{m}$, $\tilde{R}_\mathrm{s} = \hat{R}_\mathrm{s} - R_\mathrm{s}$ are the estimation errors of the stator-flux vector, rotor position, rotor speed, and stator resistance, respectively.

The local stability of the system (16) can be studied via small-signal linearization in the synchronous coordinates. An accurate stator-resistance estimate is assumed, i.e. $\tilde{R}_\mathrm{s} = 0$. When the definition (5) and the observer gain (6) are applied in (16), linearization results in

$$\frac{\mathrm{d}}{\mathrm{d}t}\begin{bmatrix}\tilde{\psi}_\mathrm{d}\\ \tilde{\psi}_\mathrm{q}\end{bmatrix} = \underbrace{\begin{bmatrix}k_{10} & -k_{10}\beta_0 + \omega_\mathrm{m0}\\ k_{20} - \omega_\mathrm{m0} & -k_{20}\beta_0\end{bmatrix}}_{\boldsymbol{A}}\begin{bmatrix}\tilde{\psi}_\mathrm{d}\\ \tilde{\psi}_\mathrm{q}\end{bmatrix} \tag{18}$$

where the operating-point quantities are marked by the subscript 0. It is worth noticing that the linearized closed-loop system is of the second order since $\tilde{\vartheta}_\mathrm{m}$ and $\tilde{\psi}_\mathrm{q}$ are linearly dependent, i.e. $\tilde{\psi}_\mathrm{q} = [\psi_\mathrm{pm} + (L_\mathrm{d} - L_\mathrm{q})i_\mathrm{d0}]\tilde{\vartheta}_\mathrm{m}$ holds.

Since accurate parameter estimates are assumed, $\tilde{\psi}_\mathrm{d0} = 0$ and $\tilde{\vartheta}_\mathrm{m0} = 0$ hold in the operating point. Therefore, the linearization is valid even if the gain scheduling is used for the observer gain. The characteristic polynomial is $\det(s\mathbf{I} - \boldsymbol{A}) = s^2 + b_0 s + c_0$, where

$$b_0 = k_{20}\beta_0 - k_{10}, \quad c_0 = \omega_\mathrm{m0}^2 - (k_{20} + k_{10}\beta_0)\omega_\mathrm{m0} \tag{19}$$

The nonlinear system (16) is locally stable if the coefficients of the characteristic polynomial are positive: $b_0 > 0$ and $c_0 > 0$. From (19), the general stabilizing gain can be solved:

$$k_{10} = -\frac{b_0 + \beta_0(c_0/\omega_\mathrm{m0} - \omega_\mathrm{m0})}{\beta_0^2 + 1} \tag{20a}$$

$$k_{20} = \frac{\beta_0 b_0 - c_0/\omega_\mathrm{m0} + \omega_\mathrm{m0}}{\beta_0^2 + 1} \tag{20b}$$

This gain is related to the closed-loop poles according to

$$s_{1,2} = \frac{-b_0 \pm \sqrt{b_0^2 - 4c_0}}{2}. \tag{21}$$

## Appendix B
## Stability of Stator-Resistance Adaptation

Assuming constant $R_\mathrm{s}$ and the stator-resistance adaptation law (11), the nonlinear dynamics of the stator-resistance estimation error become

$$\frac{\mathrm{d}\tilde{R}_\mathrm{s}}{\mathrm{d}t} = k_\mathrm{R}(\hat{\psi}_\mathrm{d} - \psi_\mathrm{pm} - L_\mathrm{d} i_\mathrm{d}) \tag{22}$$

The closed-loop system consisting of (16) and (22) can be linearized:

$$\frac{\mathrm{d}}{\mathrm{d}t}\begin{bmatrix}\tilde{\psi}_\mathrm{d}\\ \tilde{\psi}_\mathrm{q}\\ \tilde{R}_\mathrm{s}\end{bmatrix} = \begin{bmatrix}k_{10} & -k_{10}\beta_0 + \omega_\mathrm{m0} & -i_\mathrm{d0}\\ k_{20} - \omega_\mathrm{m0} & -k_{20}\beta_0 & -i_\mathrm{q0}\\ k_\mathrm{R0} & -k_\mathrm{R0}\beta_0 & 0\end{bmatrix}\begin{bmatrix}\tilde{\psi}_\mathrm{d}\\ \tilde{\psi}_\mathrm{q}\\ \tilde{R}_\mathrm{s}\end{bmatrix} \tag{23}$$

where the definition (5) and the observer gain (6) are applied. Using the Routh–Hurwitz stability criterion, the stability conditions are

$$b_0 > 0 \tag{24a}$$

$$k_\mathrm{R0}(i_\mathrm{q0} + \beta_0 i_\mathrm{d0})\omega_\mathrm{m0} > 0 \tag{24b}$$

$$k_\mathrm{R0}[(i_\mathrm{d0} - \beta_0 i_\mathrm{q0})b_0 - (i_\mathrm{q0} + \beta i_\mathrm{d0})\omega_\mathrm{m0}] + b_0 c_0 > 0 \tag{24c}$$

## Acknowledgment

The authors gratefully acknowledge the Academy of Finland and ABB Oy for the financial support.

## References

[1] G. Yang, R. Tomioka, M. Nakano, and T. H. Chin, "Position and speed sensorless control of brushless DC motor based on an adaptive observer," *IEEJ Trans. Ind. Appl.*, vol. 113, pp. 579–586, May 1993.

[2] S. Shinnaka, "New "D-state-observer"-based vector control for sensorless drive of permanent-magnet synchronous motors," *IEEE Trans. Ind. Appl.*, vol. 41, no. 3, pp. 825–833, May/June 2005.

[3] S. Koonlaboon and S. Sangwongwanich, "Sensorless control of interior permanent-magnet synchronous motors based on a fictitious permanent-magnet flux model," in *Conf. Rec. IEEE-IAS Annu. Meeting*, Hong Kong, Oct. 2005, pp. 311–318.

[4] M. Jansson, L. Harnefors, O. Wallmark, and M. Leksell, "Synchronization at startup and stable rotation reversal of sensorless nonsalient PMSM drives," *IEEE Trans. Ind. Electron.*, vol. 53, no. 2, pp. 379–387, Apr. 2006.

[5] S. Sangwongwanich, S. Suwankawin, S. Po-ngam, and S. Koonlaboon, "A unified speed estimation design framework for sensorless ac motor drives based on positive-real property," in *Proc. PCC-Nagoya'07*, Nagoya, Japan, Apr. 2007, pp. 1111–1118.

[6] J. Lee, J. Hong, K. Nam, R. Ortega, L. Praly, and A. Astolfi, "Sensorless control of surface-mount permanent-magnet synchronous motors based on a nonlinear observer," *IEEE Trans. Power Electron.*, vol. 25, no. 2, pp. 290–297, Feb. 2010.

[7] A. Piippo, M. Hinkkanen, and J. Luomi, "Sensorless control of PMSM drives using a combination of voltage model and HF signal injection," in *Conf. Rec. IEEE-IAS Annu. Meeting*, vol. 2, Seattle, WA, Oct. 2004, pp. 964–970.

[8] P. Guglielmi, M. Pastorelli, G. Pellegrino, and A. Vagati, "Position-sensorless control of permanent-magnet-assisted synchronous reluctance motor," *IEEE Trans. Ind. Appl.*, vol. 40, no. 2, pp. 615–622, Mar./Apr. 2004.

[9] A. Piippo, M. Hinkkanen, and J. Luomi, "Analysis of an adaptive observer for sensorless control of interior permanent magnet synchronous motors," *IEEE Trans. Ind. Electron.*, vol. 55, no. 2, pp. 570–576, Feb. 2008.

[10] S. D. Wilson, G. W. Jewell, and P. G. Stewart, "Resistance estimation for temperature determination in PMSMs through signal injection," in *Proc. IEEE IEMDC'05*, San Antonio, TX, May 2005, pp. 735–740.

[11] K.-W. Lee, D.-H. Jung, and I.-J. Ha, "An online identification method for both stator resistance and back-EMF coefficient of PMSMs without rotational transducers," *IEEE Trans. Ind. Electron.*, vol. 51, no. 2, pp. 507–510, Apr. 2004.

[12] K.-H. Kim, S.-K. Chung, G.-W. Moon, I.-C. Baik, and M.-J. Youn, "Parameter estimation and control for permanent magnet synchronous motor drive using model reference adaptive technique," in *Proc. IEEE IECON'95*, vol. 1, Orlando, FL, Nov. 1995, pp. 387–392.

[13] B. Nahid-Mobarakeh, F. Meibody-Tabar, and F.-M. Sargos, "Mechanical sensorless control of PMSM with online estimation of stator resistance," *IEEE Trans. Ind. Appl.*, vol. 40, no. 2, pp. 457–471, Mar./Apr. 2004.

[14] L. Harnefors, "Design and analysis of general rotor-flux-oriented vector control systems," *IEEE Trans. Ind. Electron.*, vol. 48, no. 2, pp. 383–390, Apr. 2001.